Templated Synthesis of DNA Nanotubes with Controlled Predetermined Lengths

Pik Kwan Lo, Florian Altvater and Hanadi F. Sleiman*

Department of Chemistry, McGill University, 801 Sherbrooke Street West, Montreal, QC H3A 2K6, Canada. E-mail: hanadi.sleiman@mcgill.ca

Contents

I. General

Acetic acid, boric acid, cyanogen bromide (5M in acetonitrile), formamide, 4-morpholineethanesulfonic acid (MES), $MgCl_2 \cdot 6H_2O$, StainsAll®, and tris(hydroxymethyl)aminomethane (Tris) were used as purchased from Aldrich. 5-Ethylthiotetrazole, 2000Å phosphate-CPG with a loading density of 5.4 μmol/g, and reagents used for automated DNA synthesis were purchased from ChemGenes. Exonuclease VII (ExoVII; source: recombinant), and sephadex G-25 (super fine DNA grade) were used as purchased from Amersham Biosciences. Microcon® size-exclusion centrifugal filter devices (YM10) are purchased from Millipore. RubyRed mica sheets for AFM are purchased from Electron Microscopy Sciences. Etched silicon cantilevers (OMCL-AC160TS) for AFM imaging were used as purchased from Olympus. 300 mesh copper coated carbon grids for transmission electron microscopy imaging were purchased from Electron Microscopy Sciences. Gold nanoparticles coated with citrate were purchased from Ted. Pella. Inc.

II. Instrumentation

Standard automated oligonucleotide solid-phase syntheses were performed on a Perspective Biosystems Expedite 8900 DNA synthesizer. UV/vis quantifications were conducted on a Varian Cary 300 biospectrophotometer. Gel electrophoresis experiments were carried out on an acrylamide 20 X 20 cm vertical Hoefer 600 electrophoresis unit. Electroelutions were performed using a Centrilutor® electroeluter from Millipore. Temperature controlled hybridizations were conducted using a Flexigene Techne 60 well thermocycler. AFM images were either acquired on a Digital Instruments "Dimension 3100" or on an E-scope microscope (Santa Barbara, CA).

III. Sequence of template strands 1 and 6.

All the following DNA strands were purchased from IDT Company.

Table S1 **Sequences of a, b, c, d, e and f**

	Sequence (5' - 3')
abc	TTTCGTGGTCTTTCTAACAGCAACCAGGAAGAGCT TGGAAACTATGAACTGTATATCCTTAAAACAAGAT

aabc	CGCCAATGAAGAGCGGAGTACAACCAGGAAGAGCT TGGAAACTATGAACTGTATATCCTTAAAACAAGAT
def	ACTAAATAGGTATCGAAGGTTTGTACCGAA CTTCTGCTCCTAACGATTTCAAAGCCTAGT
e'	TTCAAAGCCTAGT
a'a'	TACTCCGCTCTTCATTGGCG
a'2	CTGTTAGAAAGACCACGAAAGGCAAGTATG
a'4	CTGTTAGAAAGACCACGAAAGTGGTACGGA
a'6	CTGTTAGAAAGACCACGAAAACACAGTAGG
a'8	CTGTTAGAAAGACCACGAAACTTTACGTCC
a'10	CTGTTAGAAAGACCACGAAACTGCAATTCC
a'12	CTGTTAGAAAGACCACGAAAGATCGGATTG
a'14	CTGTTAGAAAGACCACGAAAAACAGGTGTG
a'16	CTGTTAGAAAGACCACGAAATTCACCGCGC
a'18	CTGTTAGAAAGACCACGAAACCACTGGACA
a'20	CTGTTAGAAAGACCACGAAAAAGTGCCTCC
a'22	CTGTTAGAAAGACCACGAAAGCATGAGCT T
a'24	CTGTTAGAAAGACCACGAAAGTAGCGTCTA
a'26	CTGTTAGAAAGACCACGAAACGTGCTCGAC
a'28	CTGTTAGAAAGACCACGAAATAGTAAGGCG
a'30	CTGTTAGAAAGACCACGAAACTGCCAGATT
a'32	CTGTTAGAAAGACCACGAAAAGGTCTTGGA
a'34	CTGTTAGAAAGACCACGAAAACACTCTCGT
a'36	CTGTTAGAAAGACCACGAAAGGTAGTCAGT
a'38	CTGTTAGAAAGACCACGAAACCTGAATGCG
a'40	CTGTTAGAAAGACCACGAAAGAGGTTAGCC
c'1	GCTAGATGGCATCTTGTTTTAAGGATATAC
c'3	ATACGCCGCAATCTTGTTTTAAGGATATAC
c'5	GTCCGGTAACATCTTGTTTTAAGGATATAC
c'7	TTCCACGCGAATCTTGTTTTAAGGATATAC
c'9	TGAGAAGTCCATCTTGTTTTAAGGATATAC
c'11	GATCCTCTGAATCTTGTTTTAAGGATATAC
c'13	GGACCATTACATCTTGTTTTAAGGATATAC
c'15	ACGACTCACTATCTTGTTTTAAGGATATAC
c'17	TGGATGACAGATCTTGTTTTAAGGATATAC

c'19	ACCGTCACGTATCTTGTTTTAAGGATATAC
c'21	AATGTGGCTGATCTTGTTTTAAGGATATAC
c'23	CTCCTAAGCAATCTTGTTTTAAGGATATAC
c'25	ATTGATGCCGATCTTGTTTTAAGGATATAC
c'27	CTCTACATGGATCTTGTTTTAAGGATATAC
c'29	TTCGGTTCGTATCTTGTTTTAAGGATATAC
c'31	ACAAGCGCACATCTTGTTTTAAGGATATAC
c'33	TAGCAGGCCAATCTTGTTTTAAGGATATAC
c'35	CCGAGTTGACATCTTGTTTTAAGGATATAC
c'37	ATGCACCAACATCTTGTTTTAAGGATATAC
c'39	ATGGAGCCGTATCTTGTTTTAAGGATATAC
c'41	GCGTTGTTCCATCTTGTTTTAAGGATATAC
d'1'	GCCATCTAGCACTAGGCTTTGAAATCGTTA
d'3'	TGCGGCGTATACTAGGCTTTGAAATCGTTA
d'5'	GTTACCGGACACTAGGCTTTGAAATCGTTA
d'7'	TCGCGTGGAAACTAGGCTTTGAAATCGTTA
d'9'	GGACTTCTCAACTAGGCTTTGAAATCGTTA
d'11'	TCAGAGGATCACTAGGCTTTGAAATCGTTA
d'13'	GTAATGGTCCACTAGGCTTTGAAATCGTTA
d'15'	AGTGAGTCGTACTAGGCTTTGAAATCGTTA
d'17'	CTGTCATCCAACTAGGCTTTGAAATCGTTA
d'19'	ACGTGACGGTACTAGGCTTTGAAATCGTTA
d'21'	CAGCCACATTACTAGGCTTTGAAATCGTTA
d'23'	TGCTTAGGAGACTAGGCTTTGAAATCGTTA
d'25'	CGGCATCAATACTAGGCTTTGAAATCGTTA
d'27'	CCATGTAGAGACTAGGCTTTGAAATCGTTA
d'29'	ACGAACCGAAACTAGGCTTTGAAATCGTTA
d'31'	GTGCGCTTGTACTAGGCTTTGAAATCGTTA
d'33'	TGGCCTGCTAACTAGGCTTTGAAATCGTTA
d'35'	GTCAACTCGGACTAGGCTTTGAAATCGTTA
d'37'	GTTGGTGCATACTAGGCTTTGAAATCGTTA
d'39'	ACGGCTCCATACTAGGCTTTGAAATCGTTA
d'41'	GGAACAACGCACTAGGCTTTGAAATCGTTA
f'2'	ACCTTCGATACCTATTTAGTCATACTTGCC
f'4'	ACCTTCGATACCTATTTAGTTCCGTACCAC

f'6'	ACCTTCGATACCTATTTAGTCCTACTGTGT
f'8'	ACCTTCGATACCTATTTAGTGGACGTAAAG
f'10'	ACCTTCGATACCTATTTAGTGGAATTGCAG
f'12'	ACCTTCGATACCTATTTAGTCAATCCGATC
f'14'	ACCTTCGATACCTATTTAGTCACACCTGTT
f'16'	ACCTTCGATACCTATTTAGTGCGCGGTGAA
f'18'	ACCTTCGATACCTATTTAGTTGTCCAGTGG
f'20'	ACCTTCGATACCTATTTAGTGGAGGCACTT
f'22'	ACCTTCGATACCTATTTAGTAAGCTCATGC
f'24'	ACCTTCGATACCTATTTAGTTAGACGCTAC
f'26'	ACCTTCGATACCTATTTAGTGTCGAGCACG
f'28'	ACCTTCGATACCTATTTAGTCGCCTTACTA
f'30'	ACCTTCGATACCTATTTAGTAATCTGGCAG
f'32'	ACCTTCGATACCTATTTAGTTCCAAGACCT
f'34'	ACCTTCGATACCTATTTAGTACGAGAGTGT
f'36'	ACCTTCGATACCTATTTAGTACTGACTACC
f'38'	ACCTTCGATACCTATTTAGTCGCATTCAGG
f'40'	ACCTTCGATACCTATTTAGTGGCTAACCTC
f'42'	ACCTTCGATACCTATTTAGTGGCCGACAAA
42	TTTGTCGGCC

IV. Assembly characterizations of A1 to A21, B1 to B21 and C1 to C21.

The hybridizations of **A1** to **A21** and **B1** to **B21** are monitored using 8% native PAGE, and is found to occur quantitatively for the hybridization products. Generally, 1.12 X 10^{-10} moles of each of the DNA strands, are mixed in 0.5 μL TAMg buffer (40 mM Tris, 20 mM acetic acid, 12.5 mM $MgCl_2 \cdot 6H_2O$; pH 7.8), and are left incubating at room temperature for 15 minutes. As seen in Fig. S1 and S2, the hybridization of products **A1** to **A21** (lane 3, lanes 5 to 24) and **B1** to **B21** (lanes 6 to 26), occurs quantitatively.

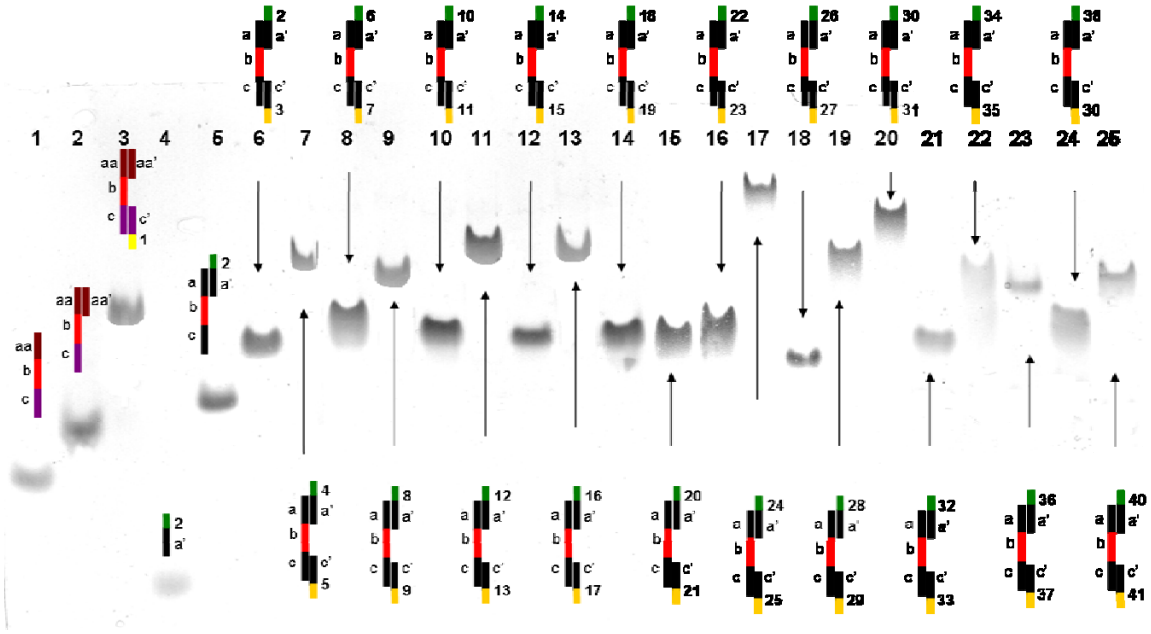

Figure S1 **Assembly of A1 to A21.** Native PAGE analysis reveals the clean hybridization products of A1 (lane 3) and **A2** to **A21** (lanes 5 to 24)

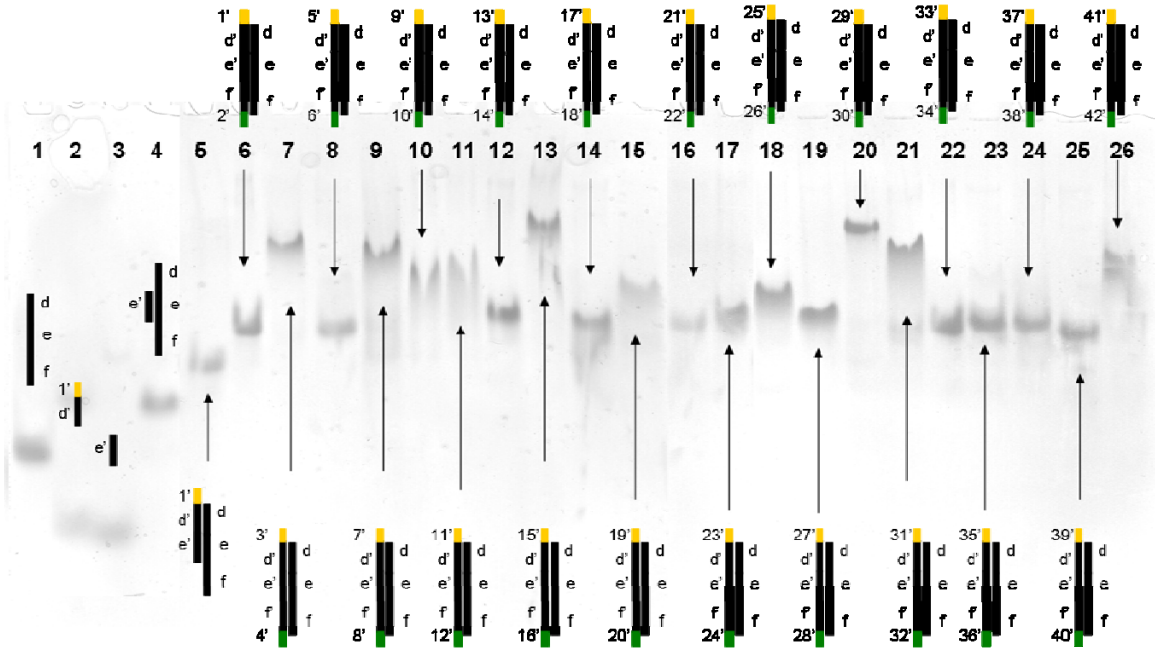

Figure S2 **Assembly of B1 to B21.** Native PAGE analysis reveals the clean hybridization products of **B1** to **B21** (lanes 6 to 26).

The corresponding **C1** to **C21** are prepared by mixing **A1** and **B1**, **A2** and **B2**, **A3** and **B3** etc…..to **A21** and **B21** respectively**,** and leaving to incubate on ice for 30 minutes. The hybridization products **C1** to **C21**, are monitored using 8% native PAGE. As seen in Fig.

S3, the hybridization of products **C1** to **C21** (lanes 5 to 25) occurs quantitatively. The final template **1** and **6** are generated by mixing **C1**, **C2**, **C3**, etc…..to **C21** and **C1**, **C2**, **C3**, etc…..to **C11** at room temperature respectively.

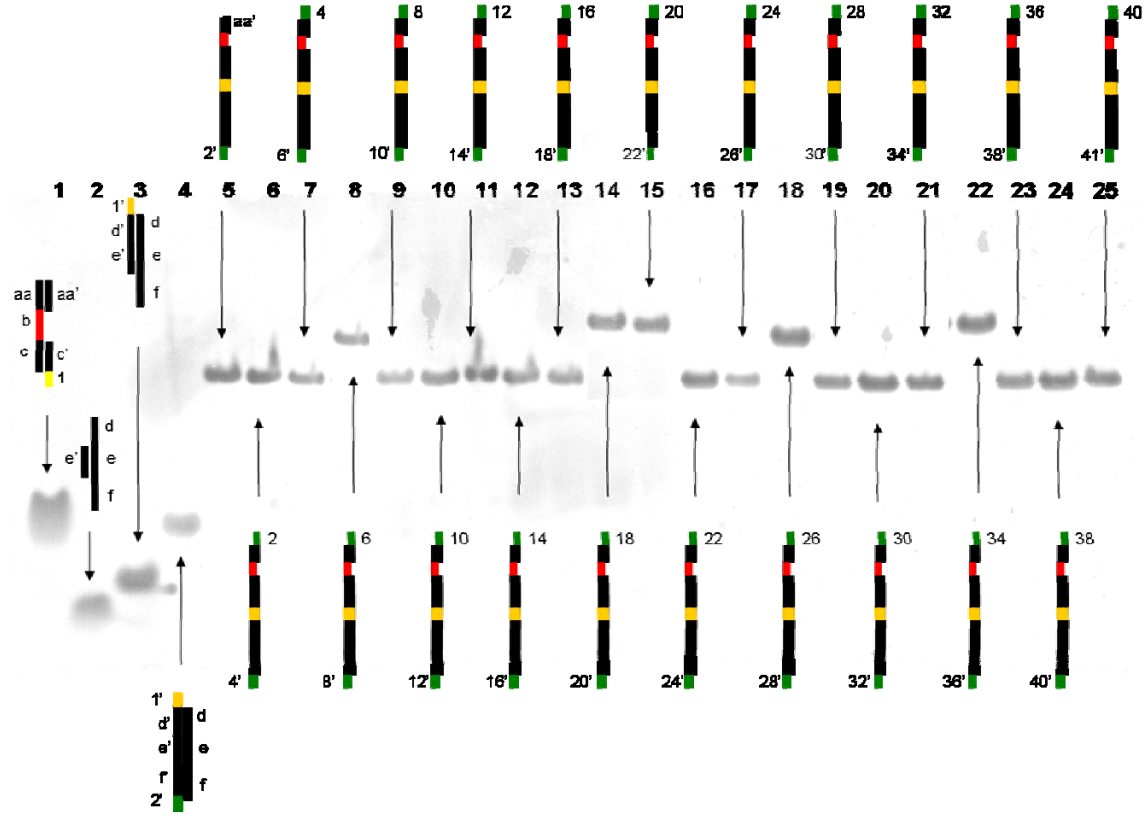

Figure S3 **Assembly of C1 to C21.** Native PAGE analysis reveals the clean hybridization products of **C1** to **C21** (lanes 5 to 25).

V. Construction of triangular rung 3 and 7

The construction of templates **2** and **9** is carried out according to a previously reported method by Sleiman and co-workers. [S1] All DNA strands are cleaved and deprotected from the solid-support in a concentrated solution of ammonium hydroxide (55 °C, 12 hrs), purified using 24% 7 M urea polyacrylamide gel electrophoresis, extracted into 3 mL of water (16 hrs, 37 °C), and desalted using Sephadex G-25 column chromatography. Quantification is carried by UV/vis analysis using Beer's law ($A_{total} = A_{vertex} + A_{DNA}$), in which the extinction coefficient of the vertex at 260 nm is calculated to be 2.30 X 10^5 L mol^{-1} cm^{-1}.

Table S2 **Sequences of CS and RS.**

	Sequence (5' - 3')
CS1	AGTTCATAGTTTCCCAAACCAATATGTCGTTTC CATAGTATTGCATGACGCTGG
CS2	CACTCTAAAAGGAACTCTTGTACCTTCAAGA GATTACTGACCAGATCGAATGTAAGTTGA
CS3	GGTTGATCTCGAAAGGCTGGCCGATTTGTGT TATTGGTCAGCTCTTCCTGGTTG
CS1'	AGTTCATAGTTTCCAATCAGTCCTCCCAGCAAACCTTTCAACCTA ATGACCAATAATAGTATTGCATGACGCTGG
CS2'	CACTCTAAAAGGAACTCTTGAACACAAATCGGCGGCAAAGATG TCGTTTCCTACCTTCAAGCCAGATCGAATGTAAGTTGA
CS3'	GGTTGATCTCGAAAGGCTGGAAGATTACTGAGATACCAATAG AAGTCACGCGAAAGGCTTCGCTCTTCCTGGTTG
RS2	GCAATACTAT TT CAAGAGTTCC
RS3	TTCGATCTGG TT CCAGCCTTTC

The construction of the triangular rung **3** and **10** is conducted using a number of complementary strands **CS** and rigidifying strands **RS** (Scheme S1). **10**, for example, is constructed from one unit of the template **9**, three complementary strands containing sticky-end overhang cohesions **CS1'-CS3'**, and from three rigidifying strands that serve to orient each of these sticky-ends into one of two lateral directions **RS2** & **RS3**.

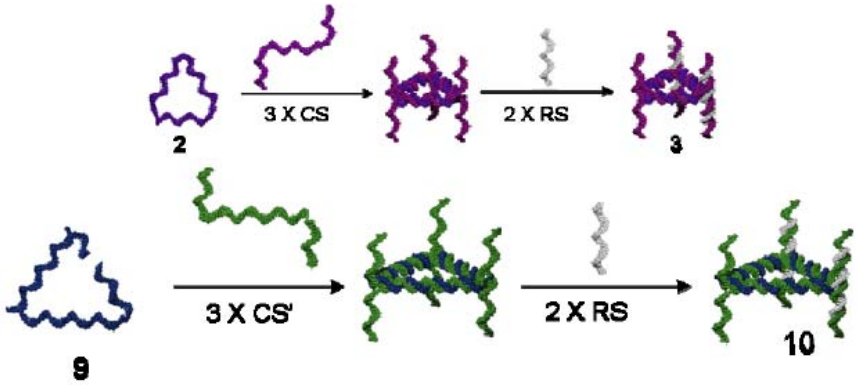

Scheme S1 **Construction of 3 and 10.**

Assemblies are typically conducted by combining all required DNA strands in the correct molar ratios (final DNA assembly of 1.2 X 10^{-10} moles per strand in 1 μL TAMg buffer), and by incubating at 70 °C for 5 minutes followed by slowly cooling to 5 °C over a period of 10 hours. Table S1 summarizes the sequences of the strands used to construct **3**

and **10** from **2** and **9**, respectively. This process is monitored sequentially and is found to occur quantitatively at each step leading to, and including, the construction of the triangular-shaped rung **3** (Fig. S1).

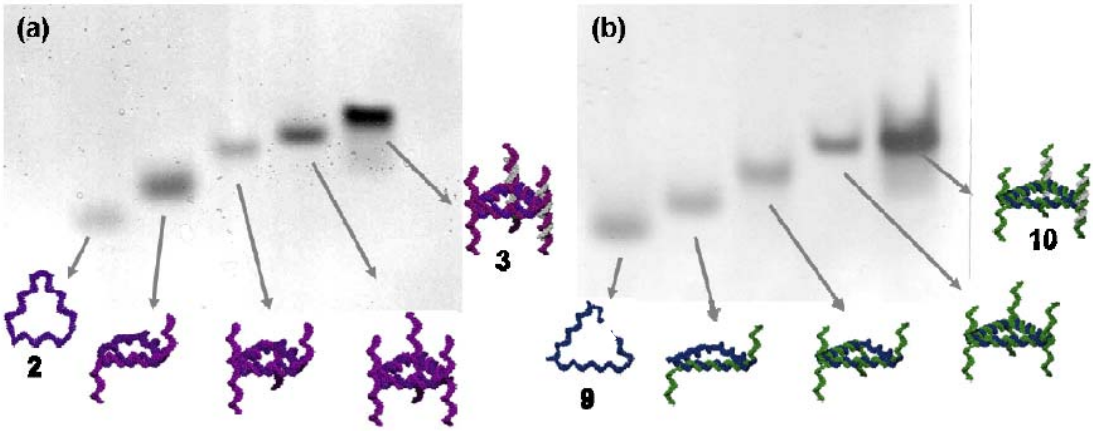

Figure S4 **Construction of 3 and 10.** (a) The single- stranded and cyclic template **2** (lane 1) is sequentially titrated with the complementary strands **CS1-CS3** (lanes 2-4, respectively), and with the **RS2-RS3** strands to quantitatively generate a fully assembled triangular rung **3** (lane 5) (b) The strand **9** (lane 1) is sequentially titrated with the complemetary strands **CS1'-CS3'** (lane 2-4, respectively), and with the **RS2&RS3** strands to quantitatively generate a fully triangular rung **10**.

VI. Assembly and characterization of DNA nanotubes 5 and 8.

(i) Assembly of small triangular shaped DNA nanotubes 5

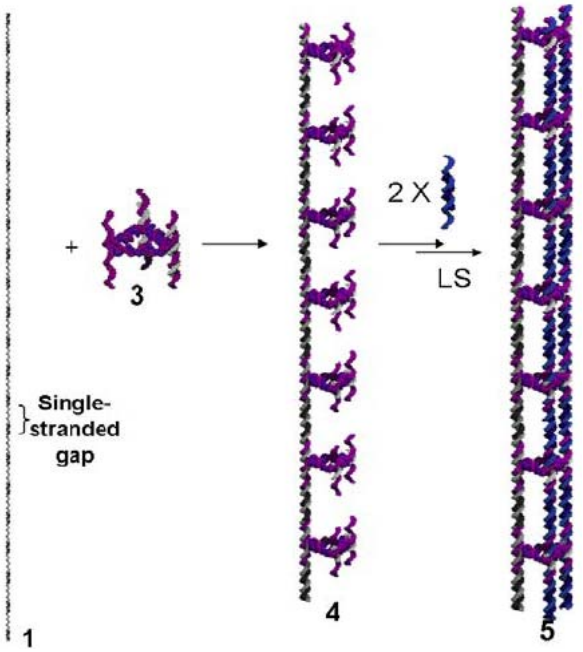

Scheme S2 **Assembly of nanotubes 5**

Assemblies are typically conducted in 2 μL of TAMg buffer, and involve addition of the pre-formed small triangular rung **3** which was heat at 70 °C, for 10 minutes, followed by slow cooling to 5 °C over a period of 10 hours, to the already assembled template **1.** After 2 hours, the double-stranded linking strands (**LS**) are added in the correct molar ratio at room temperature, to generate an assembly with a final DNA strand concentration of 4.0 X 10^{-6} mol L^{-1}. Table S3 summarizes the LS and RSLS sequences used to assemble nanotubes.

Table S3 **Sequence of LS and RSLS.**

	Sequence (5' - 3')
LS2	TTTTAGAGTGAACCTCTGGTGATTAGTACGAGGCCGATAC GTGCTAAGAATGCCGTTTTGTGGAGCCTTCCGACTGTGAG CTTTCGGTCCGGTAACCGTGGCGACACCTTGAGACAAGCC AGCGTCAT
LS3	GAGATCAACCAACCTCTGGTGATTAGTACGAGGCCGATAC GTGCTAAGAATGCCGTTTTGTGGAGCCTTCCGACTGTGAG CTTTCGGTCCGGTAACCGTGGCGACACCTTGAGACAAGTC AACTTACA
RSLS23	CTTGTCTCAAGGTGTCGCCACGGTTACCGGACCGAAAGCT CACAGTCGGAAGGCTCCACAAAACGGCATTCTTAGCACGT ATCGGCCTCGTACTAATCACCAGAGGTT

AFM sample preparation typically involves the deposition of 5 μL of the self-assembled mixture (concentration of 10 pM) onto freshly cleaved mica (dimensions 2 X 2 cm), followed by evaporation to achieve complete dryness (typically 30 mins in a fumehood). Whenever possible, imaging is conducted within 24 hours to minimize time-dependant sample degradation. AFM images are acquired in air, and at room temperature. "Tapping mode" (i.e. intermittent contact imaging) is performed at a scan rate of 1 Hz using etched silicon cantilevers with a resonance frequency of ~ 70 kHz, a spring constant of ~ 2 N/m, and a tip radius of < 10 nm. All images are acquired with medium tip oscillation damping (20-30%).

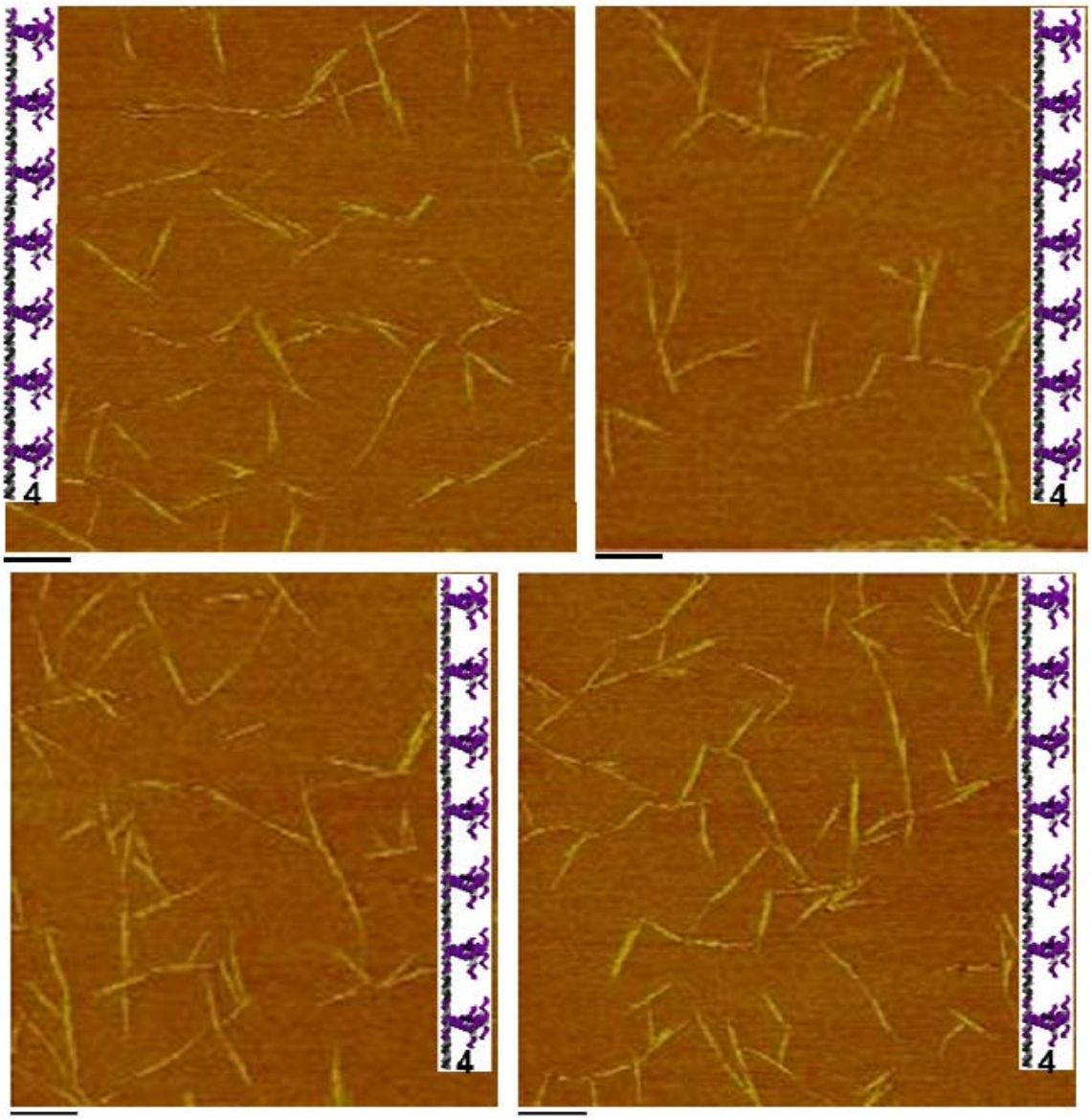

Figure S5 AFM images of assemblies **4** (Scale bar is 1μm) dried in air on mica substrate.

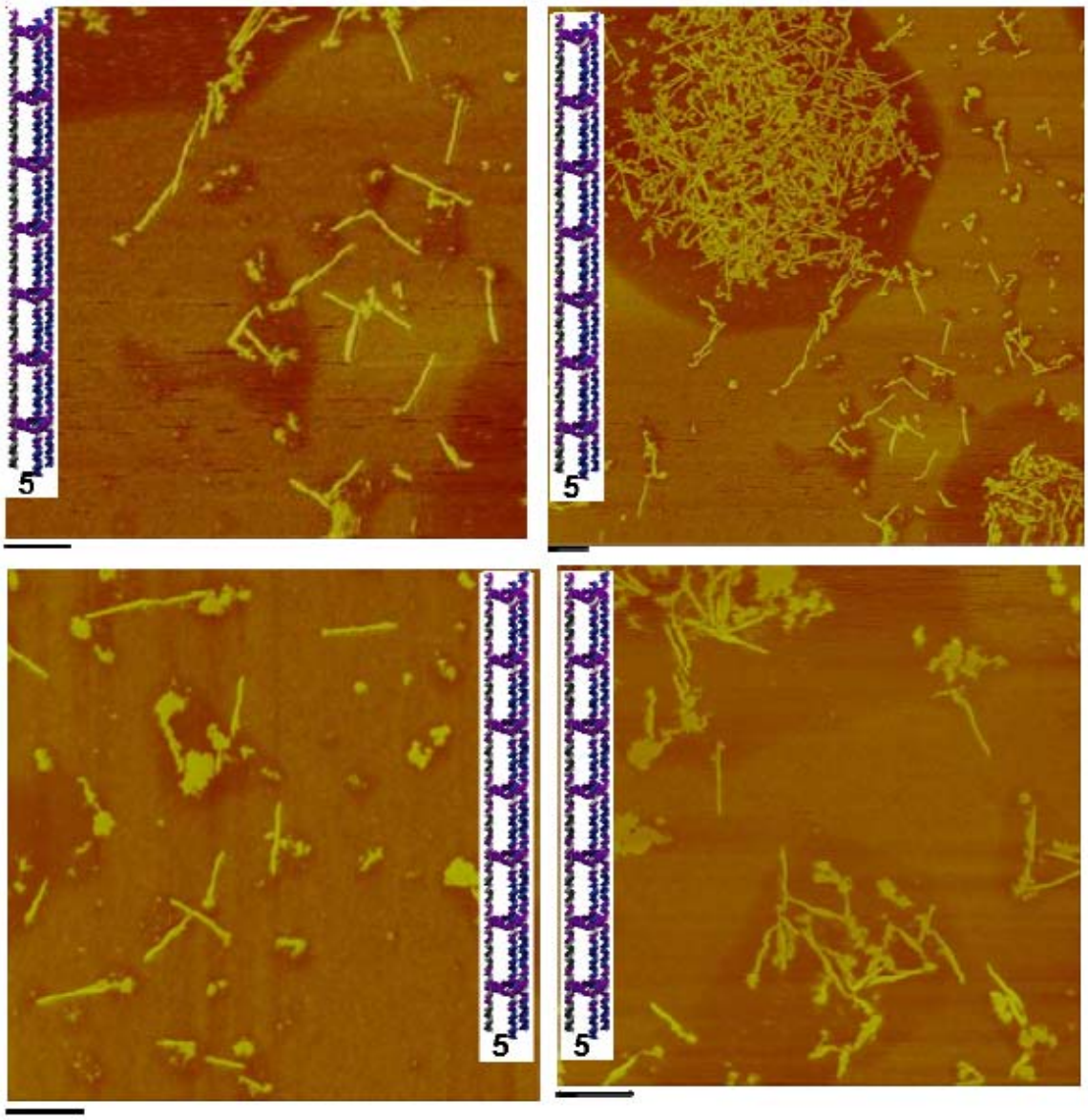

Figure S6 AFM images of nanotubes **5** (Scale bar is 1μm) dried in air on mica substrate.

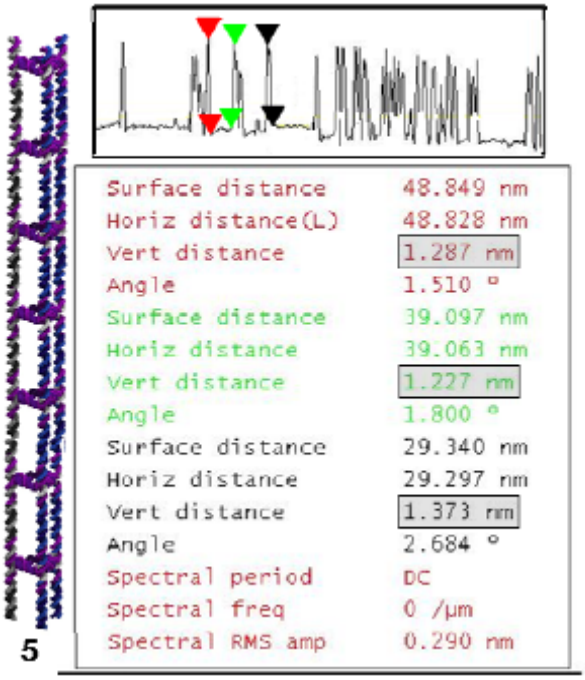

Figure S7 Height analysis of the nanotubes **5.**

A number of previous studies have shown that the height of a DNA double helix, measured by AFM is consistently lower than the expected 2 nm. Moreno-Herrero *et al.*[S2] showed that this was due to a ~0.8nm thick salt layer on mica, in which DNA strands are embedded. Chen *et al*. have recently suggested that these discrepancies are also due to tip-induced deformation of the soft DNA molecules under AFM imaging conditions, and to inconsistent-imaging dynamics, in which the cantilever oscillates in the attractive regime on substrate background but in the repulsive regime on the sample[S3]. Thus, previous AFM studies of double-stranded DNA show significantly lower heights than 2 nm.

Lateral cross-sectional analysis conducted on our nanotubes **5** show them all to be of similar height (~1.2-1.3 nm). This value is smaller than expected, likely because of the reasons outlined above, such as tip induced deformation, inconsistent imaging dynamics between the DNA sample and the mica substrate, and a salt layer on mica in which the structures are partly embedded.

(ii) **Assembly of small triangular shaped DNA nanotubes 8**

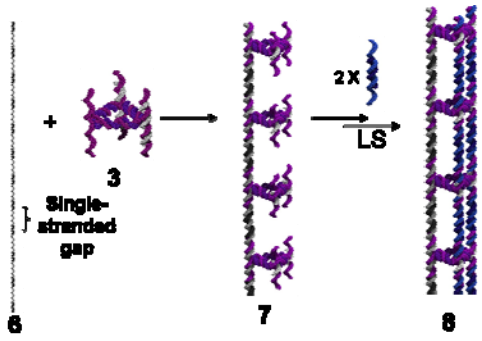

Scheme S3 **Assembly of nanotubes 8**

Assemblies are typically conducted in 2 μL of TAMg buffer, and involve addition of the pre-formed small triangular rung **3** which was heat at70 °C, for 10 minutes, followed by slow cooling to 5 °C over a period of 10 hours, to the already assembled template **6.** After 2 hours, the double-stranded linking strands (**LS**) are added in the correct molar ratio at room temperature, to generate an assembly with a final DNA strand concentration of 4.0 X 10^{-6} mol L^{-1}. Table S3 summarizes the **LS** and **RSLS** sequences used to assemble nanotubes.

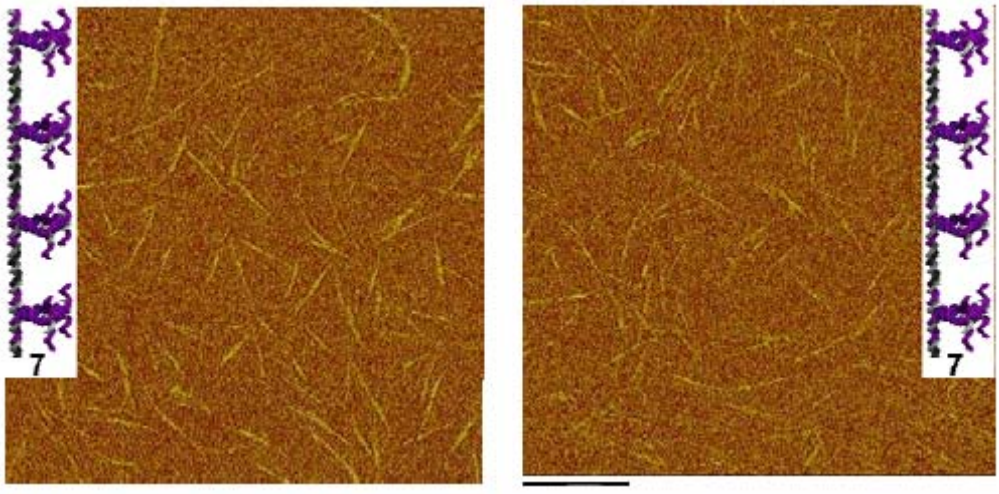

Figure S8 AFM images of assemblies **7** (Scale bar is 1μm) dried in air on mica substrate.

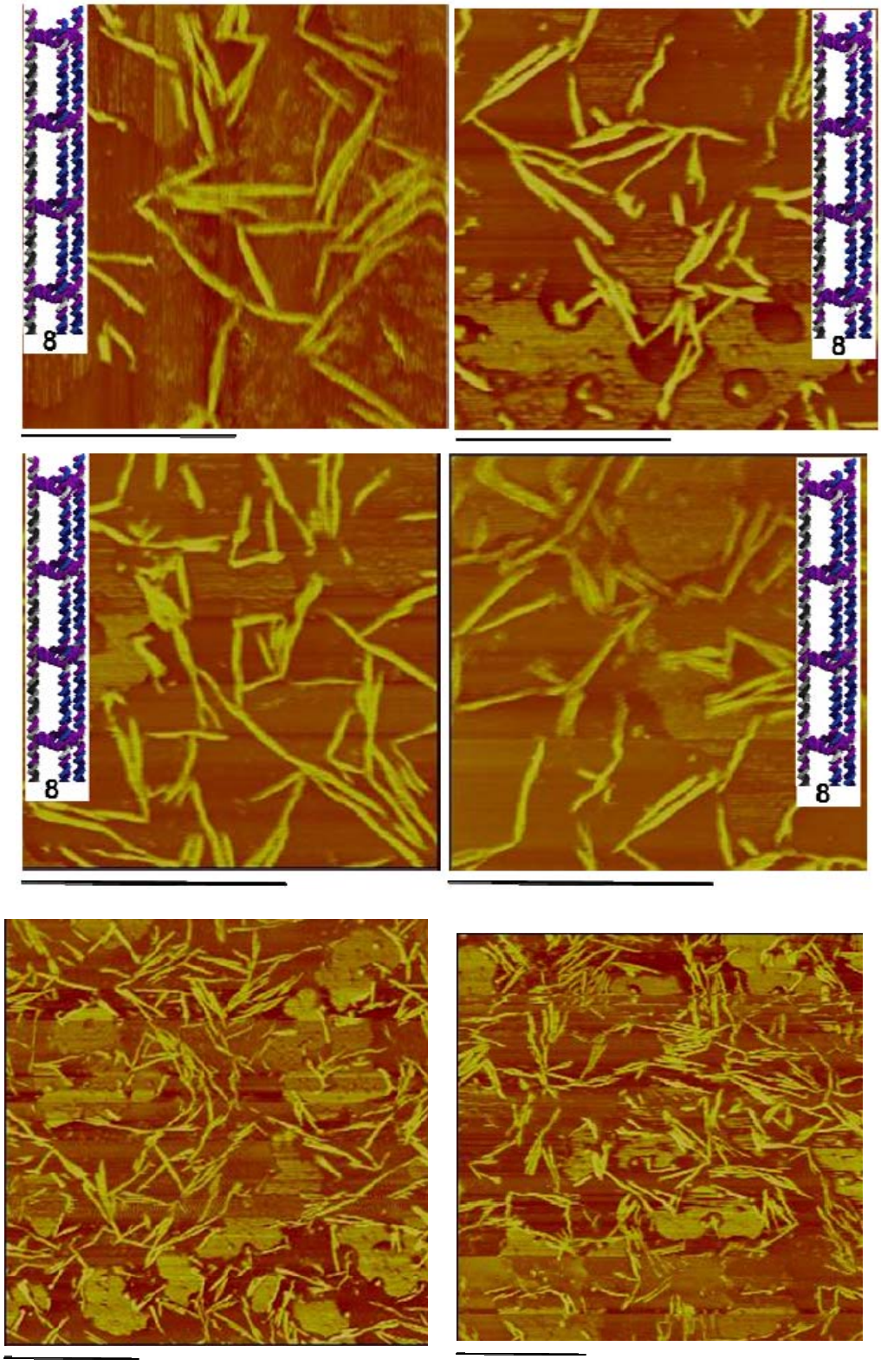

Figure S9 AFM height images of nanotubes **8** (Scale bar is 1μm) dried in air on mica substrate.

VII. Assembly and characterization of well-defined biotinylated nanotubes 5-BL and 8-BL

In our previous imaging studies, we had directly deposited our DNA structures on a mica surface with the aid of Mg^{2+} ions, and allowed the sample to air dry on this substrate. This places a sizable strain on these structures: thus, some aggregation was noted, and some structures with reduced lengths were also observed. Please note that in these studies, the percentage of structures longer than 1μm was very low. If the polydispersity were to be the result of misassembly of the DNA structures, then we would expect a significant percentage of longer, as well as shorter structures. We believe that the shorter structures are the result of shearing of these assemblies or compaction of the DNA double helices, as they are allowed to dry on the mica surface and as they interact with this highly ordered surface through Mg^{2+} bridges. Distortions arising from interactions or DNA shearing with the AFM tip are also expected.[S4]

As a result, we thought that the shearing/compaction effect during the AFM imaging process would be minimized if we introduced spacers between the mica surface and the nanotubes. We created a new template strand **1-BL**, where four biotin moieties were precisely placed on units **C2**, **C6**, **C12**, and **C18** of this template strand. This allowed the construction of 1 μm nanotubes **5-BL**, containing four biotin units per nanotube (we found that this number of biotin-labeled strands was optimal for imaging). These biotin-functionalized nanotubes were then immobilized on a streptavidin-functionalized mica surface. Thus, streptavidin units act as spacers to separate the nanotubes from the surface.

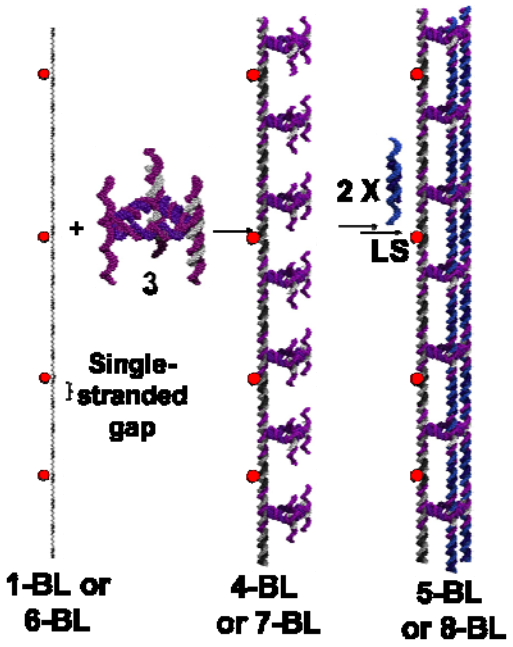

Scheme S4 **Assembly of nanotubes 5-BL or 8-BL (red dots represent the biotin groups).**

From the AFM images shown below (Figure S10), almost 85 % of the nanotubes were 0.8 to 1μm long, and shearing/shortening was thus minimized.

Figure S10 AFM height images and length statistical analysis (total number of nanotubes count = 35) of biotin-functionalized DNA nanotubes **5-BL** immobilized on streptavidin labeled mica surface. The nanotubes appear embedded within the underlying streptavidin coated substrate (Scale bar = 1μm)

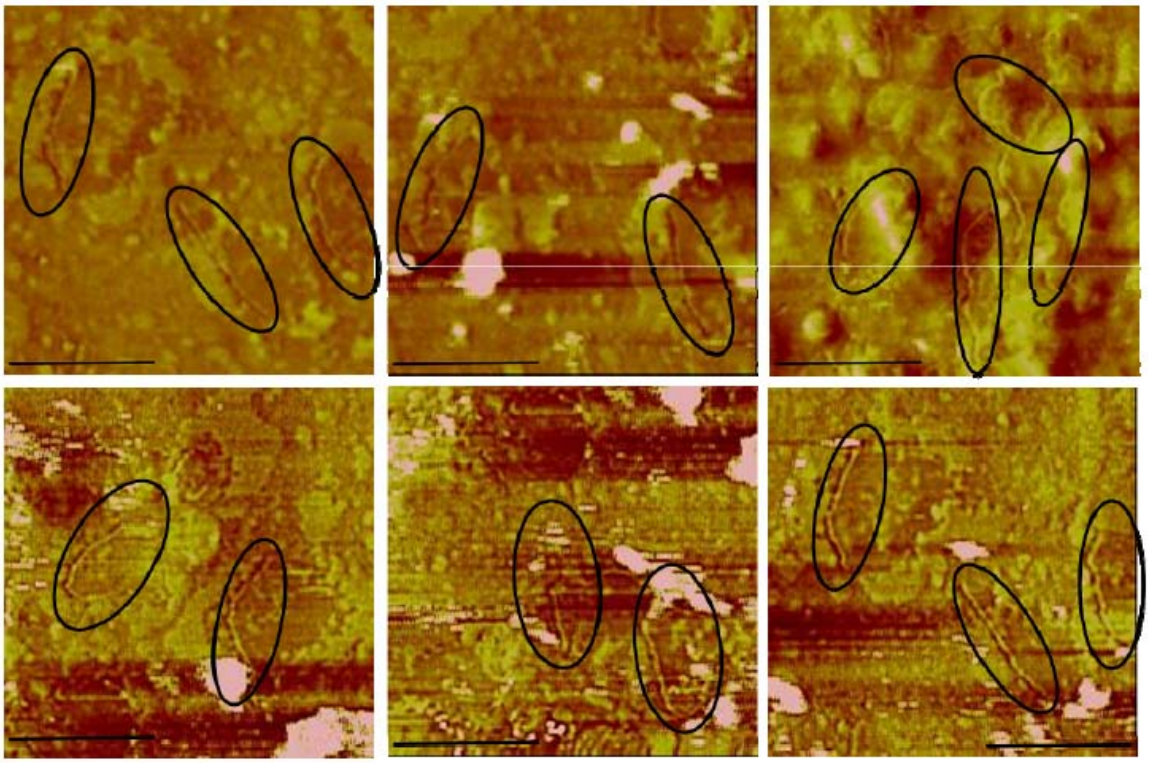

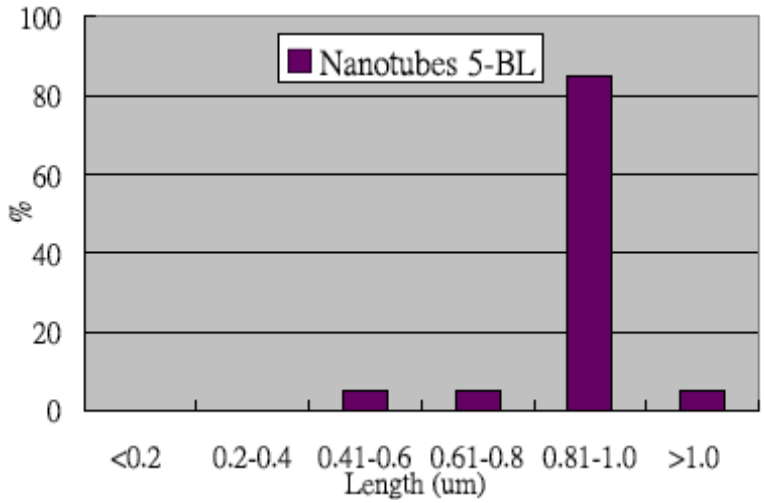

We also constructed ~0.55 μm biotin-functionalized nanotubes **8-BL** by generating template **6-BL** functionalized with two biotin units at **C2** and **C8**. Statistical length analysis conducted on individual tube **8-BL** shows a similar narrow length distribution, with a yield of approx. 78% nanotubes between 0.4 to 0.6 micron (Figure

S11). From the phase images below, one can clearly observe the association of two or more nanotubes by 'coiling together'. Interestingly, this forms a network with relatively angular features that are spaced by approx. 500 nm, ie the expected length of each nanotube. In the statistical analysis, the population of nanotubes that are longer than the template is the result of this association of the nanotubes together, as can be clearly seen by the phase images below.

Figure S11 AFM (a) phase and (b) height images, and (c) length statistical analysis (total number of nanotubes count = 180) of biotin-functionalized DNA nanotubes **8-BL** immobilized on the streptavidin labeled mica surface. (Scale bar = 500 nm)

(a)

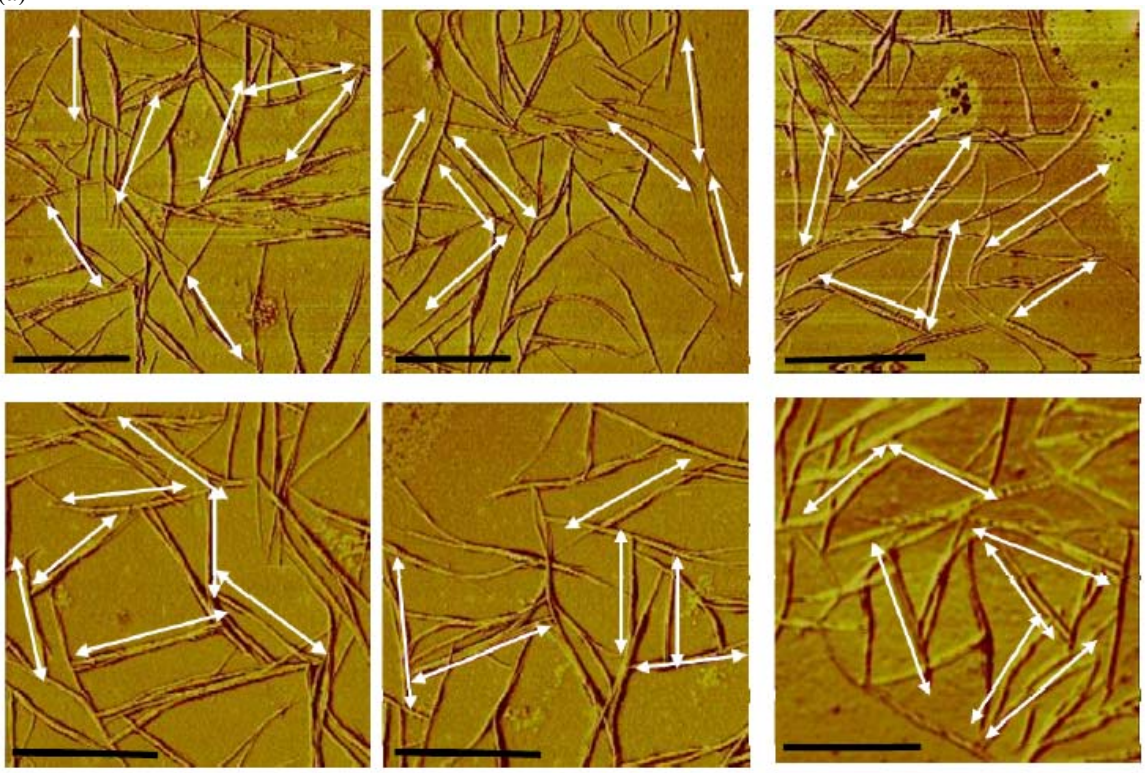

(b)

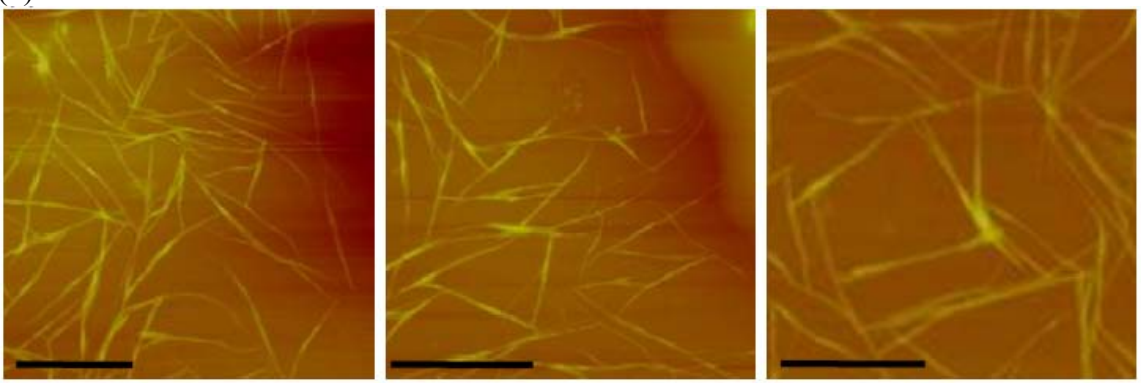

(c)

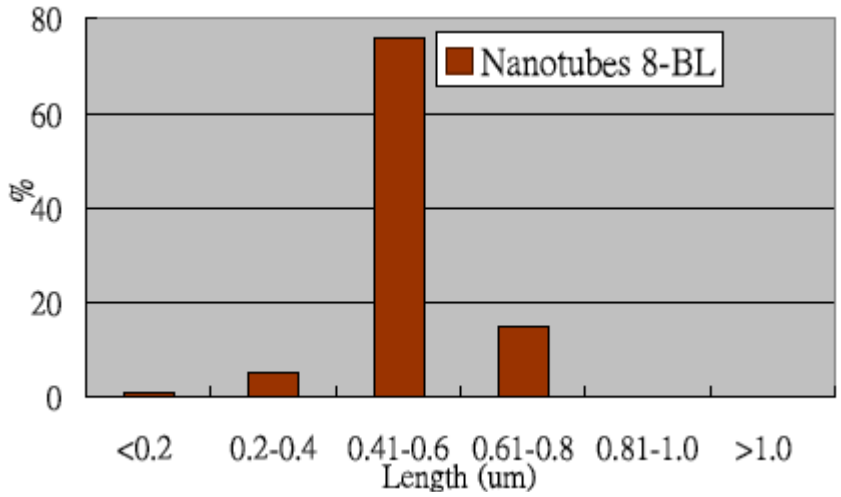

Measurements of DNA contour lengths by AFM have been shown in a number of literature reports to give significantly different results, depending on salt composition, temperature and nature of the substrate, and importantly, on whether they are carried out in air or liquid.[S5] Specifically, DNA contour lengths in air on mica substrates can be up to 20% shorter than calculated (ie, instead of 3.4 Å/base pair, they can be as short as 2.7Å/base pair). This has been explained as arising from a B- to A- DNA transition when the samples are dried in air, and by conformational changes to the DNA backbone that are induced by interaction of this backbone with the mica surface through phosphate-cation bridges. Thus, the calculated 3.4 Å /bp gives an upper limit of 1 μm for our nanotubes. In the AFM imaging experiment, we can expect up to 20% reduction in this length, or features that are about 200 nm shorter than calculated. Even for precisely defined DNA double strands, these variations have been shown to result in a distribution of contour lengths.[S5]

It is of note that the solution AFM average length of a DNA double strand is ~3.1 Å/base pair, again shorter than the theoretical value of 3.4 Å. Despite these limitations in using AFM for determining the length of our nanotubes, we have been able to obtain narrow length distributions, and 80-85% of the nanotubes were found to exhibit the two expected programmed lengths of 1μm and 0.55 μm. While deposition of samples on mica followed by air drying results in shorter lengths for these nanotubes, deposition of biotinylated nanotubes on a streptavidin-coated mica surface led to measurements that were more consistent with the expected length of these structures. Thus, these studies

have also described a new method to overcome the difficulties in measuring DNA contour lengths by AFM.

Preparation of streptavidin layer on biotin-functionalized mica

In order to prepare a layer of streptavidin molecules on mica, for incubation with biotin-functionalized DNA nanotubes, a stock solution of streptavidin (1mg/mL) in phosphate-buffered saline (PBS, 150 mM NaCl, 5mM NaH_2PO_4, pH = 7.4 adjust with NaOH) was diluted with 9 volumes of water to adjust a final streptavidin concentration of 0.1 mg/mL. The biotin-functionalized mica was incubated with diluted streptavidin solution. After one hour the mica sheet was extensively rinsed with 0.1 X PBS.

VIII. Assembly and characterization of large triangular shaped DNA nanotubes 12 and 13

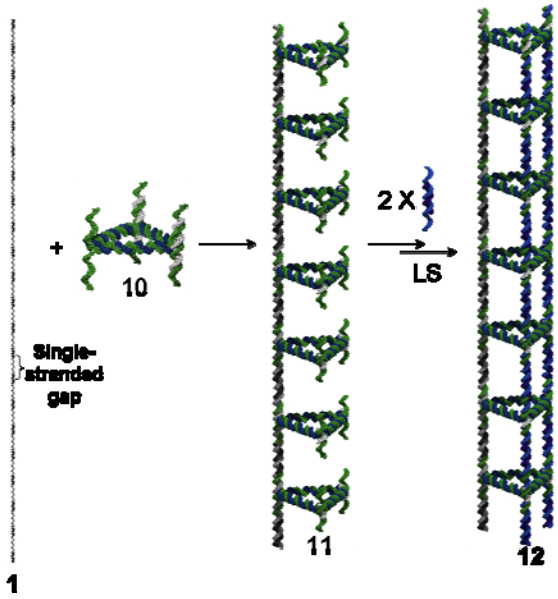

Scheme S5 **Assembly of nanotubes 12.**

Assemblies are typically conducted in 2 μL of TAMg buffer, and involve addition of the pre-formed small triangular rung **10** which was heat at 70 °C, for 10 minutes, followed by slow cooling to 5 °C over a period of 10 hours, to the already assembled template **1**. After 2 hours, the double-stranded linking strands (**LS**) are added in the correct molar ratio at room temperature, to generate an assembly with a final DNA strand concentration

of 4.0 X 10^{-6} mol L^{-1}.

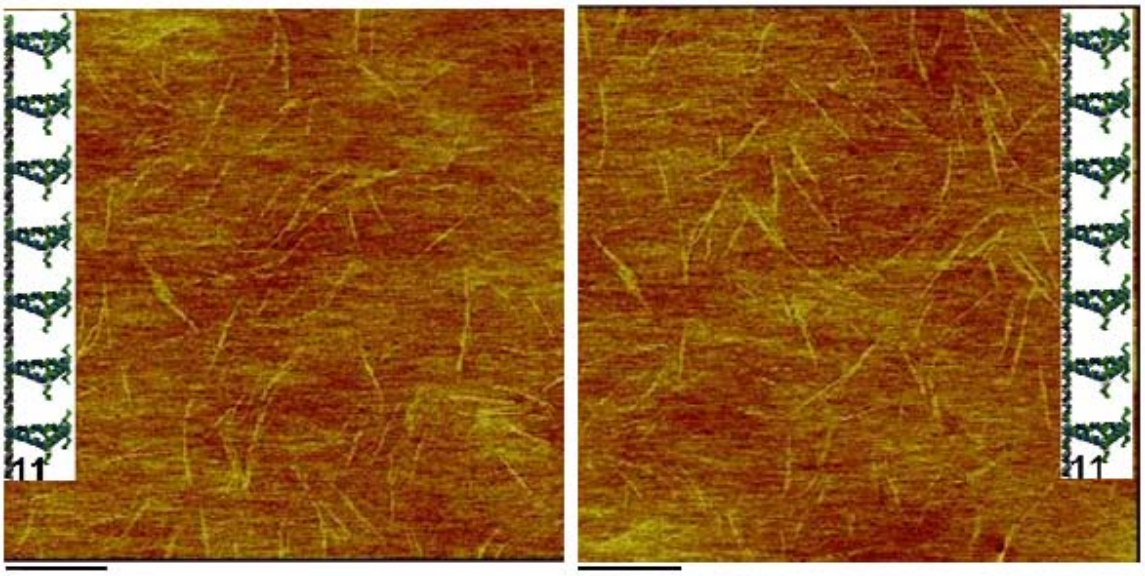

Figure S12 AFM images of assemblies **11** (Scale bar is 1μm) air-dried on mica.

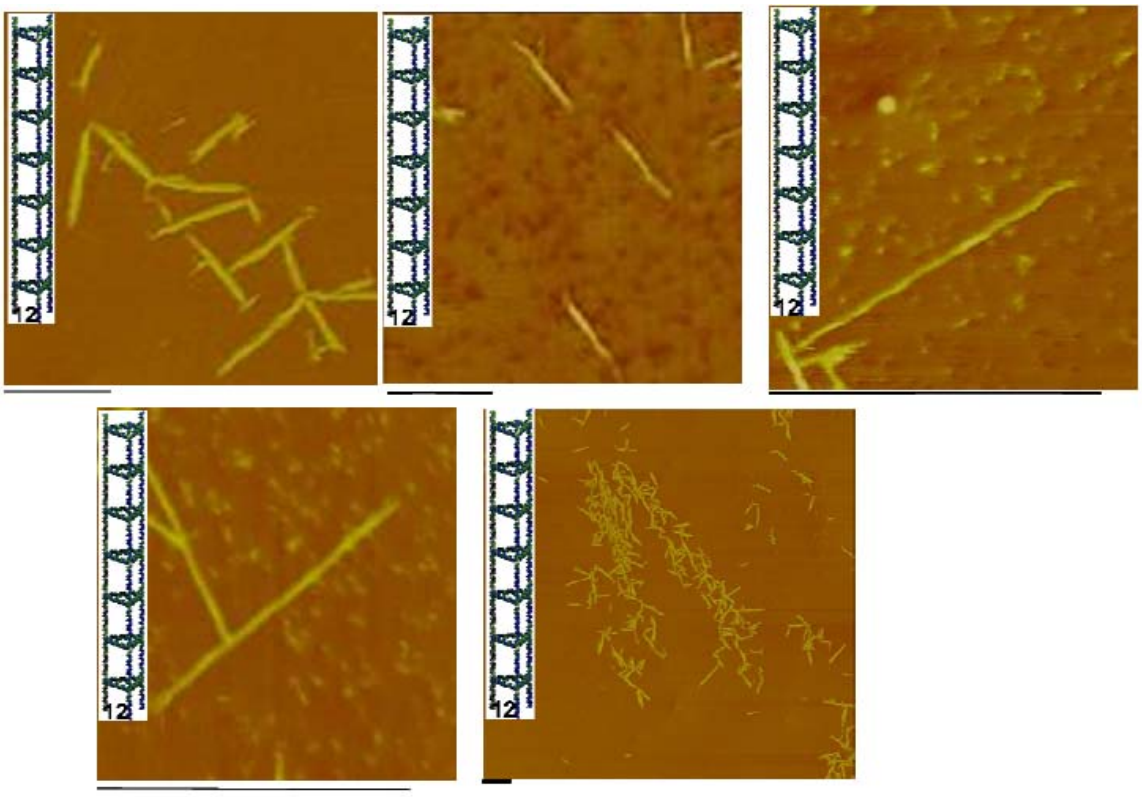

Figure S13 AFM images of nanotubes **12** (Scale bar is 1μm) air-dried on mica.

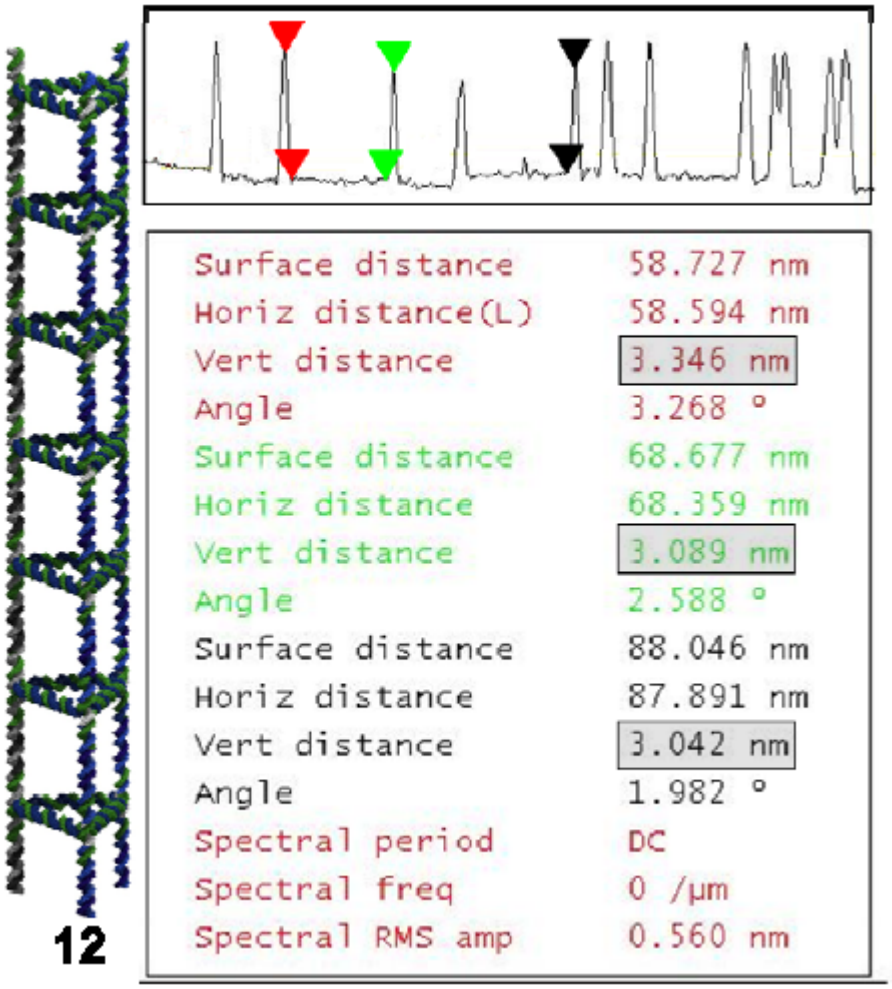

Figure S14 Height analysis of the nanotubes **12.**

Lateral cross-sectional analysis conducted on our nanotubes **12** show them all to be of the same height (~3.0-3.3 nm). This value is smaller than expected, likely because of tip induced deformation, inconsistent imaging dynamics between the DNA sample and the mica substrate, and a salt layer on mica in which the structures are partly embedded.

Assembly of large triangular shaped DNA nanotubes 13 with 20 nm gold nanoparticles

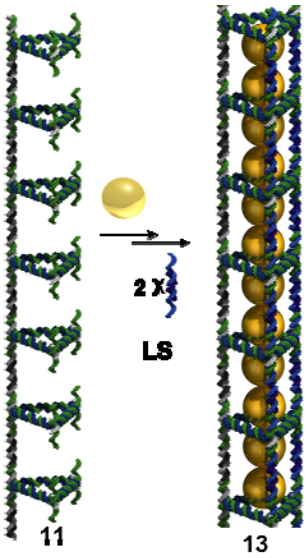

Scheme S6 **Assembly of nanotubes 13.**

Assemblies are typically conducted in 2 μL of TAMg buffer, and involve addition of the pre-formed small triangular rung **10** which was heated at 70 °C, for 10 minutes, followed by slow cooling to 5 °C over a period of 10 hours, to the already assembled template **1.** After 2 hours, the double-stranded linking strands (**LS**) and 20 nm gold nanoparticles (3:1 = AuNP:DNA per strand which is calculated by molar ratio) are added in the correct molar ratio at room temperature, to generate an assembly with a final DNA strand concentration of 4.0 X 10^{-6} mol L^{-1}.

Statistical length analysis was conducted on individual gold-encapsulated nanotubes **13**, showing a yield of approx. 65% nanotubes between 0.8 to 1 micron (Fig. 1cii in the manscript) and a reduction in the shearing/compacting effect of these tubes in the AFM scanning process. It is of note that the encapsulated nanotubes **13** retained a more rigid and stable architecture towards imaging. On the other hand, there are 15% encapsulated nanotubes longer than 1μm. We believe that this is due to the drying effect of encapsulated tubes on the mica surface and end-to-end association of the tubes together.

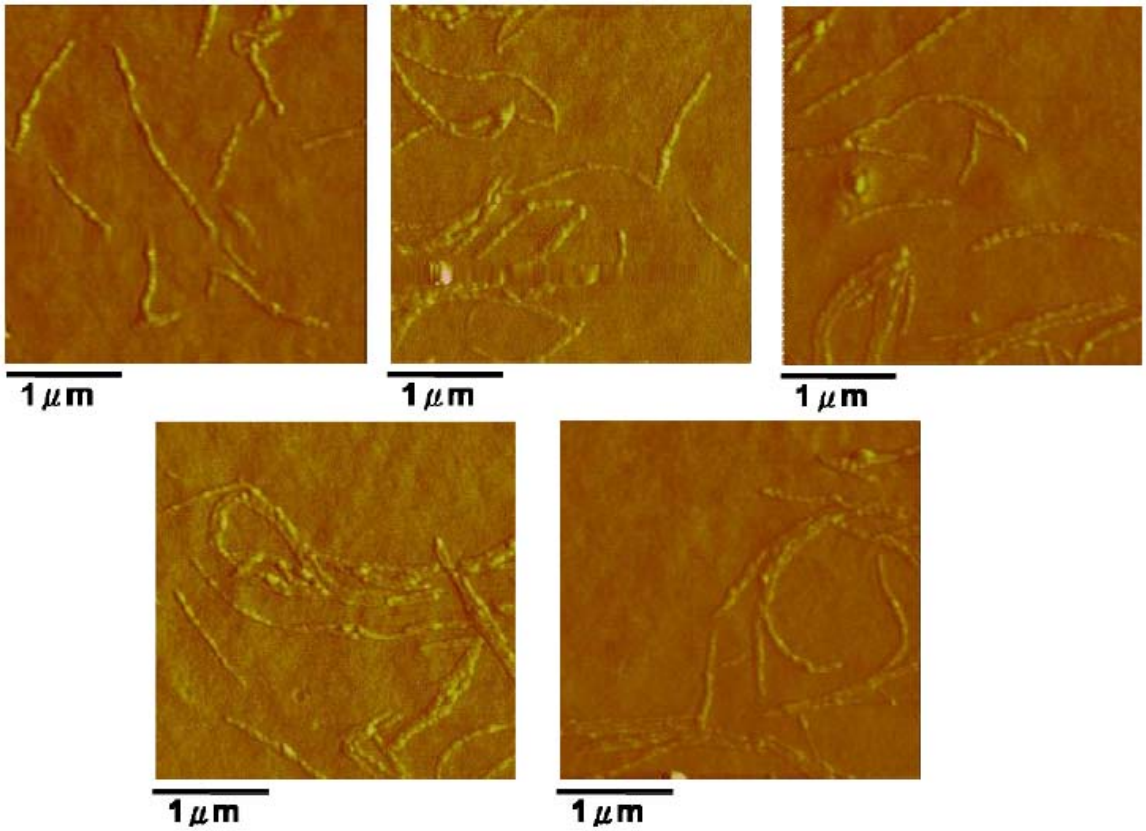

Figure S15 AFM images of nanotubes **13** (Scale bar is 1μm).

In this case, 20 nm nanoparticles are added to the nanotube **12** components, whose interior matches the nanoparticle size. As such, encapsulation and longitudinal ordering of these particles was observed, as evidenced by AFM and TEM. In addition, only in this case is a new UV/vis band at 630 nm observed, consistent with longitudinal plasmon coupling between the linear nanoparticle assemblies. Cross-sectional height analysis conducted on the raised portion of the encapsulated tubes **13** showed heights of ~6nm that are significantly greater than for the unfilled nanotubes **12**, again consistent with encapsulation of gold nanoparticles. All of these data and control experiments (see below) are consistent with selective encapsulation of the nanoparticles within our nanotubes.

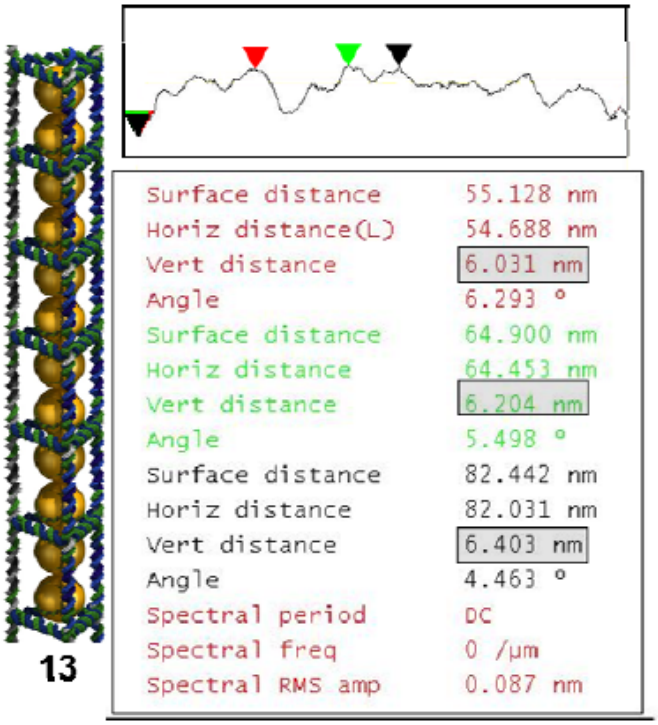

Figure S16 Height analysis of the nanotubes**13.**

IX. Control experiments to ascertain selective encapsulation

Control experiment I: When AuNPs of 10 nm average diameter were added to the nanotube components and nanotube **12** was assembled in their presence, no encapsulation was observed. This is most likely because the inner hollow space of nanotube **12** is too large to hold them in place. The capsules along the nanotube length are triangular prisms. The length of each triangle arm in these prisms is ~14 nm, and the vertical height of the prism is ~50 nm. There are thus three rectangular open faces in this large capsule, with dimensions of 14 nm X 50 nm. If the particle diameter is smaller than these values, they are likely to be able to 'escape' through these rectangular opening after they enter this capsule. Thus a 10 nm nanoparticle would not likely stay physically entrapped within these nanotubes.

Control experiment II: When 20 nm AuNP were added to only small triangular rung **3**, and these rungs were linked into a DNA nanotube with regular 7 nm cavities, no encapsulation and ordering of the particles was observed by AFM or TEM, consistent with the particles being larger than the cavities within the nanotubes. This confirms the

'sieving' capacity of these DNA nanotubes, allowing them to only effectively encapsulate nanoparticles of one unique size that matches their cavity dimensions.

Control experiment III: When the 20 nm AuNP were added to the pre-formed DNA nanotube **12**, no ordering of these particles into lines was observed, confirming that the observed particle lines indeed arise from encapsulated particles, rather than particles bound to the exterior of the DNA nanotubes.

UV/vis studies of all three control experiments showed a band at ~525 nm, but this band tailed off at higher wavelength (600 nm) in comparison to the encapsulation experiment of Figure 1civ in the manuscript.

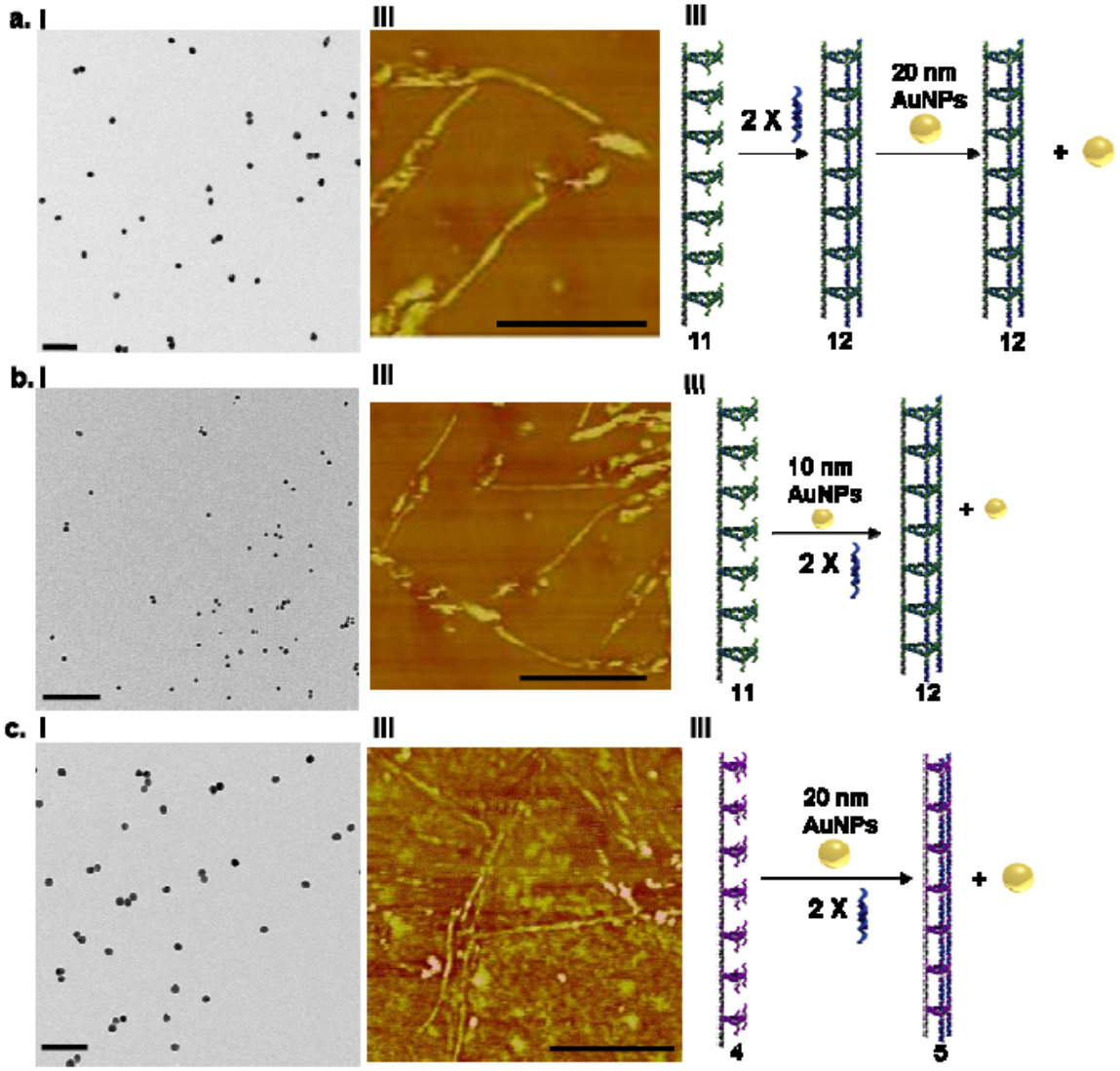

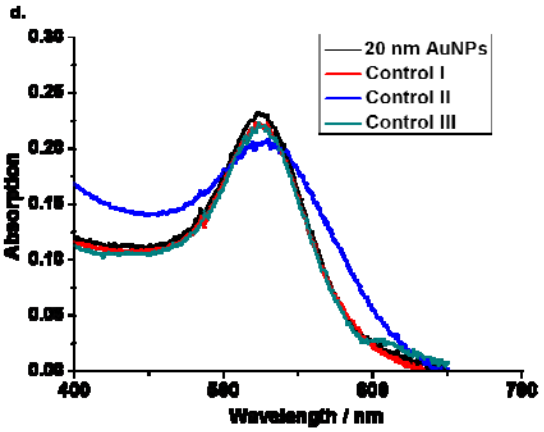

Figure S17 **Control experiments a-c**. The obtained nanoparticles and nanotubes observed by TEM (i) and AFM (ii), with the corresponding control procedure (iii) (a) 20 nm AuNPs were added to the pre-formed DNA nanotube **12**; no ordering of these particles into lines was observed, which confirmed that the observed particle lines arose from encapsulated particles, rather than from particles bound to the exterior of the DNA nanotubes. (b) AuNPs of 10 nm average diameter were added to the nanotube components and nanotube **12** was assembled in their presence; no encapsulation was observed. (c) 20 nm AuNPs were added only to the small triangular rungs **3**, and these rungs were linked into a DNA nanotube with 7 nm cavities; no encapsulation and ordering of the particles were observed. (d) The obtained nanoparticles and nanotubes observed by UV-vis studies with the corresponding control experiments I-III. Scale bars = 100 nm for TEM (i) and 1μm for AFM (ii) images.

X. References

S1. See references 8, 11, 13 in manuscript.

S2. Moreno-Herrero, F.; Colchero, J.; Baró, A. M. *Ultramicroscopy* **2003**, *96*, 167-174.

S3. Chen, L.; Yu, X.; Wang, D. *Ultramicroscopy* **2007**, *107*, 275-280.

S4. Hansma, H.G.; Vesenka, J.; Siegerist, C.; Kelderman, G.; Morrett, H.; Robert Louis Sinsheimer, V. Elings, C. *Science*, **1992**, *256*, 1180-1185.

S5. Sanchez-Sevilla, A. ; Thimonier, J. ; Marilley, M.; Rocca-Serra, J.; Barbet, J. *Ultramicroscopy* **2002**, *92*, 151-158.